

Analysis of the Electronic Exchange in Atoms*

Ingvar Lindgren

Physics Department, Yale University, New Haven, Connecticut 06520[†]

and

Karlheinz Schwarz

Quantum Theory Project, Nuclear Sciences Building, University of Florida, Gainesville, Florida 32601[‡]

(Received 25 May 1971)

The Hartree-Fock exchange and the statistical free-electron approximation are analyzed and compared for a number of atoms. The exchange energy is calculated in the two approximations—in both cases by using accurate Hartree-Fock orbitals—and split up into contributions from individual electronic shells and also into self-interaction and interelectronic parts. The results are conveniently expressed by the ratio of the various quantities in the two approximations. It is found that these parameters vary in a simple and regular way, which can be interpreted by means of an extended free-electron model. It is, e.g., found that the parameter of the total self-interaction is significantly larger than that of the total interelectronic exchange. This explains in a simple way the principal variation with the atomic number of the parameter in the so-called $X\alpha$ method. The analysis is only intended to yield some insight into the exchange phenomenon, and no new—local or nonlocal—exchange potential is suggested.

I. INTRODUCTION

Several forms of statistical exchange potentials, based on Slater's $\rho^{1/3}$ approximation¹ to the Hartree-Fock (HF) exchange, have been suggested. Such potentials have been frequently used in atomic and solid-state calculations, and extensive comparisons between the different approximations have been performed, especially in the atomic case.² It has been found that most statistical approximations reproduce the atomic HF orbitals fairly well. On the other hand, the eigenvalues of the one-electron equations are quite different in the various statistical approximations and generally in poor agreement with the HF values. However, this can be explained by a different interpretation of the eigenvalues in the statistical case.³

The most important applications of the statistical exchange approximation are in solids, where a complete HF calculation is normally prohibited for computational reasons. Furthermore, a pure HF calculation is, in general, not expected to yield results in good agreement with experiments, due to the importance of correlation (screening) effects. (One of the reasons why the statistical approach works so well for solids seems to be that it has some correlation effects automatically built into it.) In order to construct a good potential for the solid state, it is therefore necessary to have a good understanding of the exchange as well as of the correlation effects.

The purpose of the present paper is primarily to study the *exchange* effect, as a first step towards a better understanding of the statistical model. The starting point for this analysis will be the so called

" $X\alpha$ method,"⁴ in which the original Slater potential is multiplied by an adjustable constant α . Several schemes have been developed for determining the "best" values of α for atoms, and they all lead to the same general result, namely, that the "optimized" α values decrease with the atomic number Z , from about 0.8 for He to values around $\frac{2}{3}$ for heavy elements. The latter value is obtained in a straightforward way from the electron-gas theory.⁵ In the present work we shall try to explain the variation of α for low Z , using an extended electron-gas model.⁶ Our main approach to this problem will be to study the exchange *energy* in the HF and the statistical approximations. In this analysis we shall on the one hand study the exchange energy of the different shells separately and on the other hand treat the self-interaction energy separately from the remaining interelectronic exchange energy. It is our hope that such an analysis could lead to a better understanding of the exchange effect, not only for atoms, but also for molecules and solids.

II. HARTREE-FOCK AND STATISTICAL EXCHANGE ENERGY

In the HF case, we define the exchange energy by⁷

$$E_X^{\text{HF}} = \frac{1}{2} \sum_i \int \rho_i(1) U_i^{\text{HF}}(1) d\tau_1, \quad (1)$$

where U_i^{HF} is the HF exchange potential

$$U_i^{\text{HF}}(1) = -\frac{1}{\rho_i(1)} \sum_j \int \phi_i^*(1) \phi_j^*(2) \frac{1}{r_{12}} \phi_j(1) \phi_i(2) d\tau_2. \quad (2)$$

Here $\{\phi_i\}$ are the HF spin orbitals and $\rho_i(1) = |\phi_i(1)|^2$. (Since $i=j$ is included in the summation, this exchange energy contains the self-interaction.)

The exchange energy is essentially a weighted average of the exchange potential and is therefore a useful quantity for the present purpose. One disadvantage with this procedure is that possible differences in the spatial variation of the exchange energy density between various approximations may not be discovered. We shall compensate for this shortcoming by splitting up the exchange energy in several parts. This gives us a few well-defined numerical quantities to compare, rather than a set of curves.

In a free-electron gas we know that the exchange potential is approximately given by¹

$$U_s^{\text{FE}} = -2(6/\pi)^{1/3} F(\eta) \rho_s^{1/3}, \quad (3)$$

where

$$F(\eta) = \frac{1}{2} + \frac{1-\eta^2}{4\eta} \ln\left(\frac{1+\eta}{1-\eta}\right)$$

and

$$\eta = k/k_F.$$

ρ_s is here the density of electrons of a certain spin orientation and other symbols have their usual meanings. (In the non-spin-polarized case, ρ_s is equal to $\frac{1}{2}\rho$, where ρ is the total electron density.) Replacing $F(\eta)$ in this expression by its average over the occupied Fermi sphere (at zero temperature), $\langle F(\eta) \rangle = \frac{3}{4}$, leads to the original Slater exchange potential¹

$$U_s^{\text{XS}} = \langle U_s^{\text{FE}} \rangle = -\frac{3}{2}(6/\pi)^{1/3} \rho_s^{1/3}. \quad (4)$$

In the $X\alpha$ scheme⁴ one introduces an adjustable parameter α and defines

$$U_s^{X\alpha} = \frac{3}{2} \alpha U_s^{\text{XS}} = -\frac{9}{4} \alpha (6/\pi)^{1/3} \rho_s^{1/3}, \quad (5)$$

so that $U_s^{X\alpha}$ agrees with U_s^{XS} for $\alpha = \frac{2}{3}$. The variational principle then leads to the exchange potential

$$V_s^{X\alpha} = \frac{2}{3} U_s^{X\alpha} = \alpha U_s^{\text{XS}} \quad (6)$$

to be used in the one-electron Schrödinger equation. Originally, α was introduced as a parameter in this last equation, which explains the factor $\frac{3}{2}$ in the definition of $U_s^{X\alpha}$ in Eq. (5). We shall use the same parameter in our analysis, although a new parameter $\beta = \frac{3}{2}\alpha$, would be more logical.

III. CHOICE OF α VALUES

Several methods for optimizing α have been suggested and used to calculate the "best" single α values for a number of atoms. The first method to be used was to minimize the expectation value of the HF Hamiltonian using $X\alpha$ or equivalent orbitals⁸ (leading to an α value here denoted by α_{min}). Alternatively, one can equalize the statistical $X\alpha$ energy and the HF energy⁹ (α_{HF}) or satisfy the HF ex-

pression of the virial theorem by use of $X\alpha$ orbitals¹⁰ (α_{vt}). In this paper, since we are specifically interested in the exchange, we shall determine α by making the exchange energies equal in the HF and $X\alpha$ schemes, i. e.,

$$E_X^{\text{HF}} = E_X^{X\alpha} = \frac{1}{2} \int \sum_s \rho_s(1) U_s^{X\alpha}(1) d\tau_1, \quad (7)$$

and denote the corresponding α value by α_X .

The three values α_{vt} , α_{HF} , and α_X , determined by using the corresponding self-consistent $X\alpha$ orbitals, are found to be very similar, but somewhat different from α_{min} .⁹ If we neglect the difference in the orbitals between $X\alpha$ and HF, the three former values would be identical. In order to eliminate effects of differences in the orbitals, we shall use HF orbitals throughout this analysis. Then $E_X^{X\alpha}$ becomes linear in α , and α_X can be expressed by

$$\alpha_X = \frac{2}{3} E_X^{\text{HF}} / E_X^{\text{XS}}, \quad (8)$$

where

$$E_X^{\text{XS}} = \frac{1}{2} \int \sum_s \rho_s(1) U_s^{\text{XS}}(1) d\tau_1, \quad (9)$$

and U_s^{XS} is given by Eq. (4). This is the quantity we will use in the following treatment. (The effect of spin polarization will be neglected in all our numerical applications.) The numerical difference between the α_X values determined in this way and the α_{HF} and α_{vt} values, previously determined by one of the authors using self-consistent $X\alpha$ orbitals,⁹ is of the order of a few parts in 10 000 and therefore negligible from a practical point of view.

IV. EXCHANGE ENERGY FOR DIFFERENT SHELLS

The parameter α_{HF} as a function of atomic number Z is illustrated in Fig. 1 (taken from Ref. 9). These values reproduce the shell structure of the atoms very nicely and, for a given shell, α varies almost linearly with Z and is always decreasing. It is desirable to find an explanation for this kind of variation of α with Z . Since the shell structure seems to be rather important, we have separated the exchange energy into contributions from the different shells in the following way:

$$E_X^{\text{HF}} = \frac{1}{2} \sum_i \epsilon_X^{\text{HF}}(i), \quad \epsilon_X^{\text{HF}}(i) = \int \rho_i(1) U_i^{\text{HF}}(1) d\tau_1, \quad (10)$$

and correspondingly for $X\alpha$. We can now define an α parameter for each shell by requiring that $\epsilon_X^{X\alpha}(i) = \epsilon_X^{\text{HF}}(i)$. This leads to

$$\alpha(i) = \frac{2 \epsilon_X^{\text{HF}}(i)}{3 \epsilon_X^{\text{XS}}(i)} = \frac{2 \int \rho_i(1) U_i^{\text{HF}}(1) d\tau_1}{3 \int \rho_i(1) U_i^{\text{XS}}(1) d\tau_1} \quad (11)$$

in analogy with Eq. (8).

Individual α values for each shell have been calculated for a number of atoms, and the results are illustrated in Fig. 2. The values for atoms with closed subshells are given in Table I. It is found

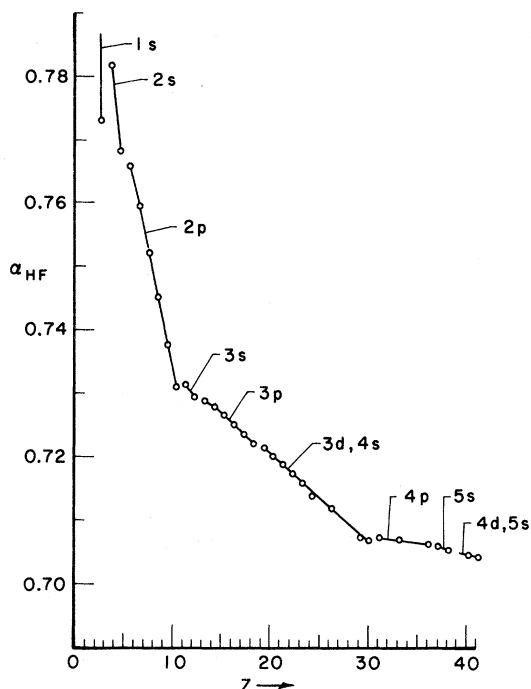


FIG. 1. Parameter in the $X\alpha$ method vs atomic number, determined by equalizing the Hartree-Fock and statistical total energies.

that $\alpha(i)$ varies smoothly with Z and is affected essentially when the main shell (K, L, M, \dots) containing the subshell i is built up. The fact that these α values are almost independent of the occupation number of outer shells shows clearly how dominant the exchange *within* the main shells is over exchange *between* such shells. It is also observed that the curves for shells with the same orbital

quantum number l have the same general shape, e. g., $2s-3s$, $2p-3p$. The s curves are essentially increasing and the p curves essentially decreasing, when the corresponding s, p shells are being filled. For the M shell it is interesting to notice that $\alpha(3p)$ increases, while $\alpha(3s)$ is essentially constant, when the $3d$ shell is being filled. It seems to be a general tendency that the α value for one subshell increases when the subshell with the next higher l value, within the same main shell, is being filled, and stays essentially constant thereafter (see Table I, e. g., $2s$ Be-Ne, $3s$ Mg-Ar, $3p$ Ca-Cu⁺). For completely filled *main* shells, the $\alpha(i)$ values are almost independent of the main quantum number n and depend essentially only on the l quantum number $\{\alpha(i) \approx 0.75-0.77$ for s electrons, $\approx 0.67-0.70$ for p electrons, $\approx 0.60-0.62$ for d electrons etc.} This general behavior can be explained by considering the self-interaction and the interelectronic exchange separately, as will be shown in Sec. V.

V. SELF-INTERACTION AND INTERELECTRONIC EXCHANGE

In the HF scheme we can separate the potential (2) into a self-interaction (SI) part

$$U_{SI}^{HF}(i) = - \int [\rho_i(2)/r_{12}] d\tau_2 \quad (12)$$

and an interelectronic exchange (IE) part

$$U_{IE}^{HF}(i) = - \frac{1}{\rho_i(1)} \sum_{j \neq i} \int \varphi_i^*(1) \varphi_j^*(2) \frac{1}{r_{12}} \varphi_j(1) \varphi_i(2) d\tau_2 \quad (13)$$

The corresponding quantities E_{SI}^{HF} and E_{IE}^{HF} are defined in analogy with Eq. (1).

As a first step in this analysis we shall investigate the correlation between the α_X values, defined in Sec. IV [Eq. (8)], and the relative magnitude of

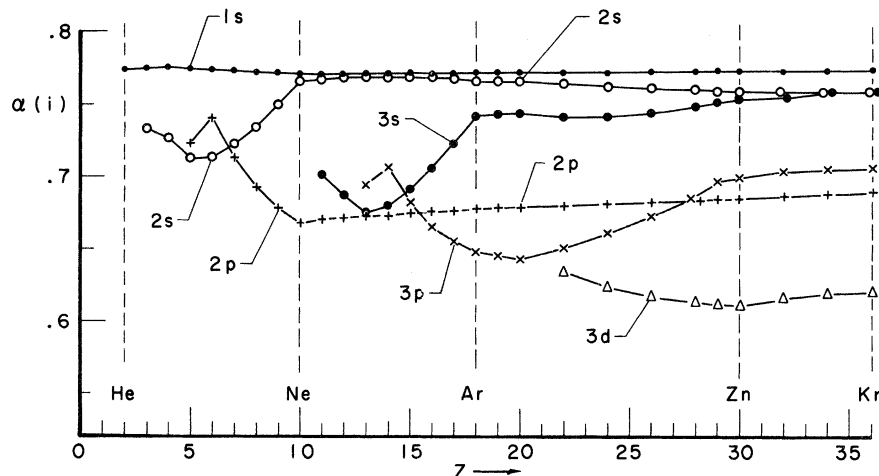


FIG. 2. Total exchange parameters for individual shells vs atomic number.

TABLE I. α values for total exchange.

Z	Average	1s	2s	2p	3s	3p	3d	4s	4p
2 He	0.7735	0.7735							
4 Be	0.7688	0.7760	0.7271						
10 Ne	0.7316	0.7709	0.7660	0.6683					
12 Mg	0.7297	0.7708	0.7693	0.6719	0.6874				
18 Ar	0.7222	0.7714	0.7664	0.6778	0.7418	0.6484			
20 Ca	0.7202	0.7717	0.7658	0.6791	0.7439	0.6436		0.6602	
29 Cu ⁺	0.7079	0.7724	0.7587	0.6837	0.7504	0.6970	0.6079		
30 Zn	0.7072	0.7726	0.7587	0.6844	0.7533	0.6986	0.6104	0.6257	
36 Kr	0.7060	0.7730	0.7583	0.6890	0.7584	0.7059	0.6204	0.7089	0.6356

the SI and IE parts of the exchange energy. Figure 3 shows the ratio of the IE and the total exchange energies vs Z for some atoms. The variation of this quantity shows a remarkable resemblance with that of the optimized single α values in Fig. 1. If we plot these α values vs the relative magnitude of the IE exchange, as shown in Fig. 4, we find a nearly linear relationship. This fact indicates very strongly that the explanation to the Z dependence of the optimized α values is to be found in the interplay between the self-interaction and the interelectronic exchange in the atoms.

In order to make an analysis analogous to that in Sec. IV, we have to split also the statistical exchange expression [Eq. (4)] into SI and IE parts. This is less straightforward than in the HF case. For that purpose we have to look closer at the uniform electron-gas model. For electrons with uniform distribution within a sphere and zero density outside, one easily finds by means of elementary

electrostatics that the average SI potential is

$$U_{SI}^{FE}(i) = -\frac{6}{5} \left(\frac{4}{3}\pi\right)^{1/3} \rho_i^{1/3}. \quad (14)$$

For electrons with less uniform distribution, like atomic electrons, one finds that the SI potential is still well described by an expression of the same type, but with a numerically slightly larger coefficient. As will be illustrated below, this coefficient is quite insensitive to changes in the distribution.

A more detailed analysis¹¹ shows that the IE potential in the free-electron model is given by

$$U_{IE}^{FE}(i) = -2(6/\pi)^{1/3} [F(\eta_i)\rho_s^{1/3} - a\rho_i^{1/3}]. \quad (15)$$

a is here a constant close to unity for $\rho_s \gg \rho_i$ and approaching $F(\eta_i)$ when $\rho_s \rightarrow \rho_i$, since IE vanishes in this limit. [It should be observed that the expression above is *not* obtained from the conventional expression (3) by subtracting some kind of self-interaction, but is obtained from the free-electron model by studying the interelectronic exchange di-

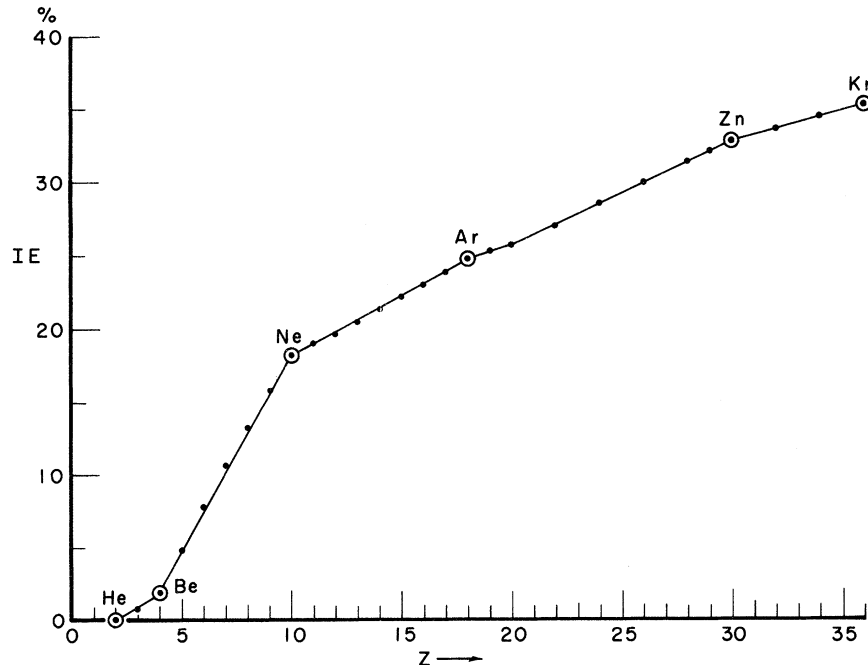


FIG. 3. Magnitude of the interelectronic exchange energy (relative to the total exchange energy) vs atomic number.

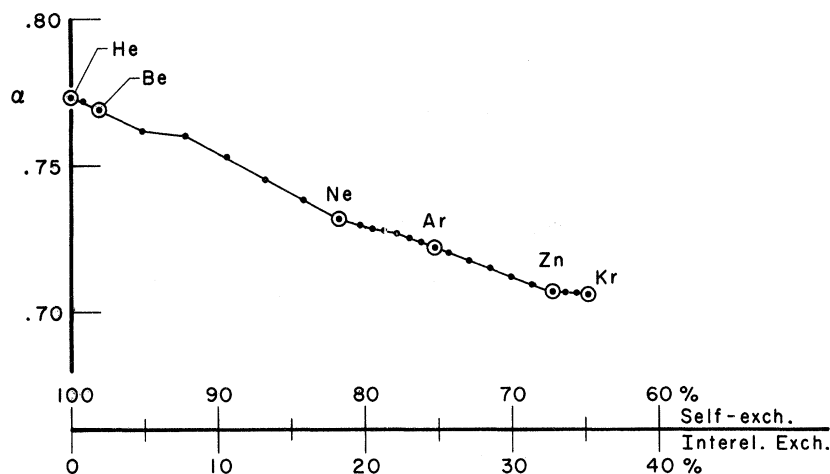


FIG. 4. Parameter for the total exchange (\approx the parameter in the $X\alpha$ method) vs the relative magnitude of the self-interaction and interelectronic exchange energies.

rectly.] The coefficients of the $\rho_i^{1/3}$ terms in Eqs. (14) and (15) are numerically not very different, which means that Eq. (3) is a reasonably good approximation of the *total* exchange—including self-interaction—also when ρ_s is not very much larger than ρ_i , i. e., when the self-interaction is not negligible. However, the coefficients are not exactly equal, which causes a significant difference between the conventional expression Eq. (3) and the sum of the more accurate expressions Eqs. (14) and (15), when ρ_i and ρ_s are comparable, i. e., when the SI forms a substantial part of the total exchange. In this case we have approximately $a \approx F(\eta_i)$, which gives

$$U_{IE}^{FE}(i) = -2(6/\pi)^{1/3} F(\eta_i)(\rho_s^{1/3} - \rho_i^{1/3}) \quad (16)$$

with the average

$$\langle U_{IE}^{FE}(i) \rangle = -\frac{3}{2}(6/\pi)^{1/3}(\rho_s^{1/3} - \rho_i^{1/3}). \quad (17)$$

This is the interelectronic potential used in the recently suggested "Hartree-Slater" method.¹¹

If we add the SI potential (14) (with a coefficient corresponding to typical atomic orbitals) to the IE potential (17), we find that the total exchange potential in the limit of large SI becomes approximately

$$\langle U^{FE}(i) \rangle = U_{SI}^{FE}(i) + \langle U_{IE}^{FE}(i) \rangle \approx U_s^{XS} + 0.15 U_{SI}^{FE}(i), \quad (18)$$

where the Slater potential U_s^{XS} is given by Eq. (4). Therefore, in this limit only about 85% of the SI is included in the conventional Slater expression. These very simple arguments explain why the optimized α values are larger than $\frac{2}{3}$ for light atoms

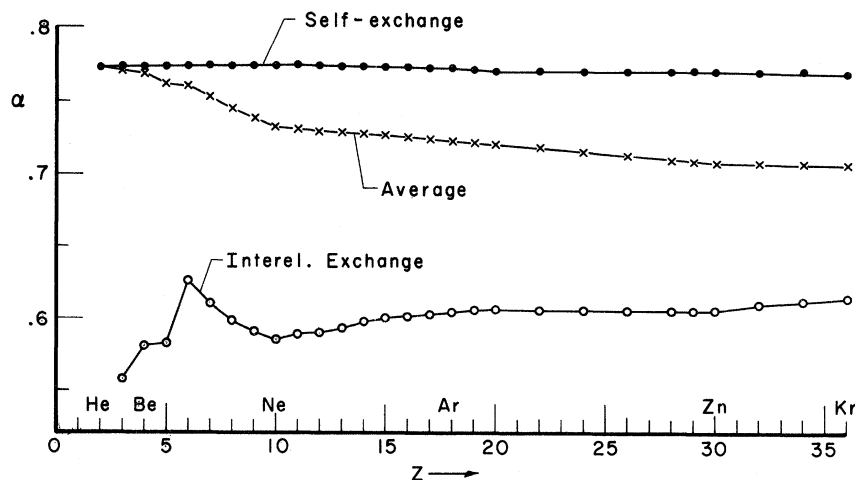


FIG. 5. Parameters for self-interaction and interelectronic exchange vs atomic number. The "average" values are the same as in Figs. 1 and 4.

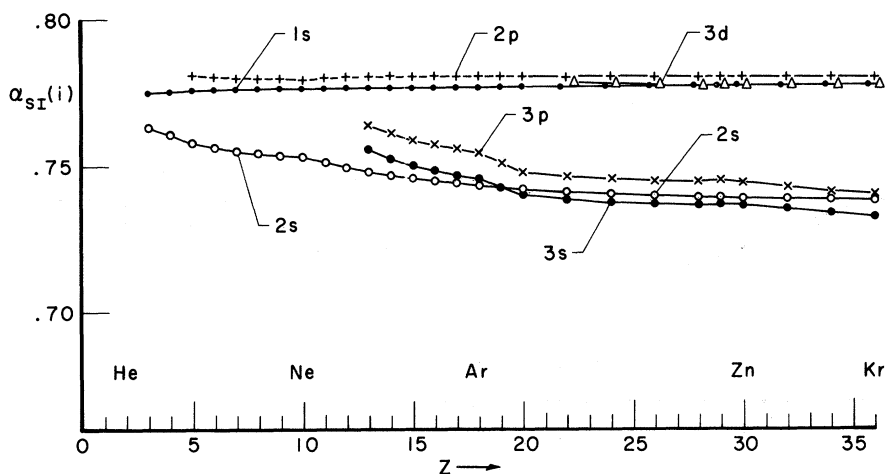


FIG. 6. Self-interaction parameters for individual shells vs atomic number.

(by roughly 15%) and approach the latter value when Z increases and SI becomes less important. The expression (18) also explains qualitatively the linear relation between α and the relative magnitude of the self-interaction in the region where the latter dominates, as illustrated in Fig. 4.

For a more quantitative analysis we need unique definitions of the SI and IE parts of the statistical exchange (4). For that purpose we adopt the expression (17) as the definition of IE in this case

$$U_{IE}^{XS}(i) = \langle U_{IE}^{FE}(i) \rangle \quad (19)$$

and consequently get the remaining part

$$U_{SI}^{XS}(i) = -\frac{3}{2}(6/\pi)^{1/3} \rho_i^{1/3} \quad (20)$$

as the SI part of the statistical potential. [Note, that this differs from the expression (14).] We can now split up the statistical exchange energy (9) into SI and IE parts and make the same analysis as before for the two parts separately by comparing them with the corresponding HF expressions defined above [see Eqs. (12) and (13)]. We can express the results by means of separate α factors for SI and IE, as illustrated in Fig. 5. There one immediately ob-

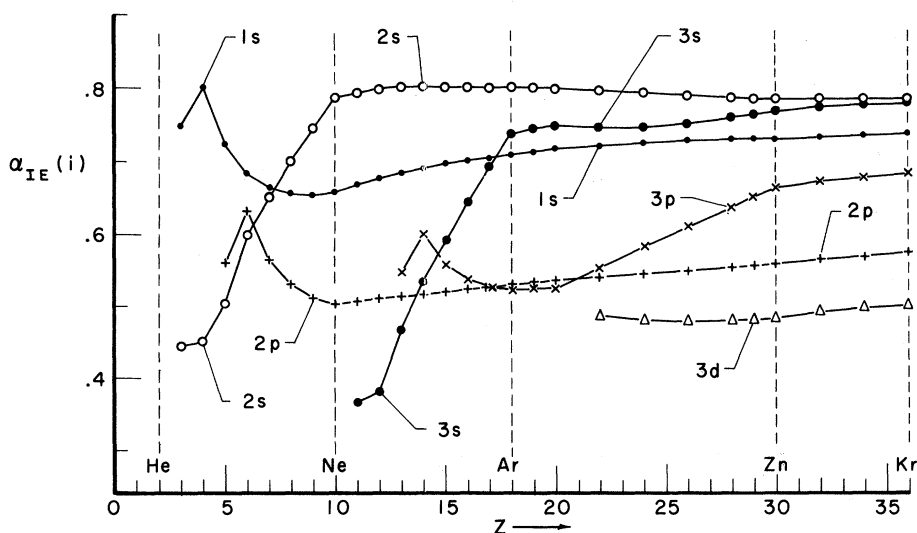


FIG. 7. Interelectronic exchange parameters for individual shells vs atomic number.

TABLE II. α values for interelectronic exchange.

Z	Average	1s	2s	2p	3s	3p	3d	4s	4p
4 Be	0.5804	0.8011	0.4550						
10 Ne	0.5857	0.6588	0.7856	0.5031					
12 Mg	0.5905	0.6764	0.7983	0.5107	0.3822				
18 Ar	0.6040	0.7082	0.7985	0.5306	0.7373	0.5235			
20 Ca	0.6058	0.7157	0.7982	0.5358	0.7486	0.5259		0.3626	
29 Cu [*]	0.6052	0.7295	0.7838	0.5548	0.7614	0.6585	0.4779		
30 Zn	0.6055	0.7309	0.7838	0.5575	0.7669	0.6625	0.4828	0.3532	
36 Kr	0.6136	0.7377	0.7831	0.5726	0.7784	0.6803	0.5005	0.6737	0.5181

serves that this leads to two quite different α factors, both essentially independent of Z . This result is, of course, not very surprising in view of the qualitative analysis made above. The two α factors obtained from Fig. 5 are

$$\alpha_{\text{SI}} \approx 0.77 \text{ and } \alpha_{\text{IE}} \approx 0.60,$$

which is reasonably close to what one expects from the simple model, discussed above [Eq. (18)], namely,

$$\alpha_{\text{SI}}^{\text{FE}} \sim 0.8 \text{ and } \alpha_{\text{IE}}^{\text{FE}} \sim 0.67.$$

We can also separate the SI and IE energies into contributions from the different shells, in the same manner as before, and define corresponding α values. The result of this analysis is illustrated on Figs. 6 and 7 and in Table II. This shows again that the SI parameters are almost independent of Z and, furthermore, essentially the same for all shells. Almost all values for $Z \leq 36$ are confined to the region $0.74 \leq \alpha \leq 0.78$. This demonstrates clearly how insensitive the self-interaction is to the shape of the electron distribution, as was briefly mentioned above. It is interesting to compare these values with that obtained for a uniform electron distribution. From Eq. (14) one finds that this corresponds to an α value of

$$\alpha_{\text{SI}}^{\text{FE}} = 0.693.$$

Thus, the SI parameters for atomic orbitals are some 10% larger than this FE value. One also finds from Fig. 6 that orbitals with a single maximum (1s, 2p, 3d, ...) have larger α_{SI} values than have orbitals with several maxima or minima (2s, 3s, 3p, ...). This is consistent with the fact that the latter electrons are less localized and hence should be closer to the FE limit.

The corresponding interelectronic parameters $\alpha_{\text{IE}}(i)$ (Fig. 7 and Table II) show the same tendency as the $\alpha(i)$ parameters discussed above (Fig. 2 and Table I), namely that they vary markedly when the main shell containing the subshell i is being filled, and remain essentially constant when outer shells are built up. One also notices that the α_{IE} values for each main shell span approximately the same range, ≈ 0.5 – 0.8 , with the α values decreasing

with l . This can be explained if we look upon the expression for IE in the FE model [Eq. (16)] before the averaging of $F(\eta)$ is being made. If we compare this expression with Eq. (17), which is our reference, we get the ratio

$$U_{\text{IE}}^{\text{FE}}(i) / \langle U_{\text{IE}}^{\text{FE}}(i) \rangle = \frac{4}{3} F(\eta_i). \quad (21)$$

According to our notations, this corresponds to an α value of

$$\alpha_{\text{IE}}^{\text{FE}}(i) = \frac{2}{3} \frac{4}{3} F(\eta_i), \quad (22)$$

which lies in the region 0.44 to 0.89. The α factors calculated from HF are consequently in good general agreement with this simple picture. The variation with l within this range can be understood, if we consider that the electron interaction is strongest within the main shells, where the overlaps are largest. Within one main shell, the electrons with the smaller l value have the lower energy and hence would correspond to a smaller k value in the free-electron model, i. e., to a larger $F(\eta)$ factor in Eq. (3).

We are now in position to explain the main variation of the $\alpha(i)$ parameters, shown in Fig. 2 and Table I. The fact that the interaction is strongest within the main shells explains why the α values of one main shell change most when that shell is being built up, but are essentially unaffected by the filling of outer main shells. Since the parameter for SI is larger than that for IE, we can also understand why the $\alpha(i)$ parameter for one subshell decreases, when that particular subshell is being filled, and consequently, SI plays a relatively smaller and smaller role. The FE model also explains why the α values for a certain subshell increases when subshells with higher angular momenta within the same main shell are being filled. This is due to the l dependence of the IE exchange, discussed above (see Fig. 7 and Table II).

It is interesting to look at the absolute magnitude of the various parts of the exchange energy. The different contributions are tabulated in Table III for a few atomic systems. This demonstrates how dominant the exchange energy of the inner shells is—particularly the self-interaction—also for relatively heavy atoms. Therefore, the α factor given above

TABLE III. Absolute exchange energies.

Z	Total	1s	2s	2p	3s	3p	3d	4s	4p
2 He SI	1.026	1.026							
IE							
10 Ne SI	9.90	5.97	1.02	2.90					
IE	2.21	0.25	0.70	1.26					
18 Ar SI	22.71	10.92	2.20	7.32	0.64	1.64			
IE	7.48	0.83	1.70	3.47	0.51	0.97			
29 Cu ⁺ SI	44.41	17.77	3.81	13.20	1.24	3.58	4.81		
IE	21.27	1.71	3.19	7.01	1.57	3.95	3.84		
36 Kr SI	60.77	22.13	4.83	16.91	1.67	4.99	8.30	0.55	1.39
IE	33.08	2.32	4.28	9.68	2.32	6.05	6.97	0.50	0.95

for the *total* exchange, which is essentially the parameter used in the $X\alpha$ method, depends almost entirely on the exchange of inner shells and reflects only to a very small extent the behavior of the outer electrons. At this stage we shall not draw any further conclusions from this fact, but we believe that this point is worth considering, when potentials for molecules or crystals are constructed.

VI. SUMMARY AND CONCLUSIONS

In this work we have tried to analyze the Hartree-Fock exchange interaction for atoms in terms of the statistical approximation. The general tool has been to divide up the HF exchange energy into parts corresponding to individual shells, as well as into self-interaction and interelectronic parts, and compare the various parts with the corresponding quantities in an extended free-electron model. It is found in this way that the HF exchange for atoms exhibits a remarkably simple and clear picture, which can be easily interpreted—to some extent also quantitatively—by the FE model employed. It is felt that this kind of analysis gives a better understanding of the exchange problem than do analyses in terms of one or two more or less arbitrary parameters. We have chosen to make our analysis by means of a number of parameters, defined in analogy with the α value in the frequently used $X\alpha$ meth-

od. However, it should be emphasized that this is only a formal way of describing the results. Our treatment is by no means intended to be an extension of the $X\alpha$ method, and we do not suggest any multiparameter potential. The analysis is merely to be considered as a step towards a better understanding of the exchange effect along somewhat different lines than are normally followed in related works. It is our hope that this might be of value when accurate calculations on molecules and solids are planned. Needless to say, in such cases one has to consider also the important effect of electron correlation, which has not been the concern of us in this work.

ACKNOWLEDGMENTS

The authors are grateful to Professor John Slater for his interest in this work and for his support. They also want to express their thanks to Professor Per-Olov Löwdin and other members of the Quantum Theory Project for stimulating discussions. One of the authors (I. L.) wishes to thank Professor Vernon Hughes for his hospitality during the stay at Yale University. The calculations have been carried out on the IBM 360/65 computer at the University of Florida Computing Center and at the IBM 7094/7044 computer at the Yale University Computing Center.

*Work partially supported by the National Science Foundation Grant No. GP-16464 and the U.S. Air Force Contract No. F44260-70-0091.

†On leave from Chalmers University of Technology, Göteborg, Sweden.

‡On leave from the Institut für Physikalische Chemie der Universität Wien, Vienna, Austria.

¹J. S. Slater, Phys. Rev. **81**, 385 (1951); *Quantum Theory of Atomic Structure* (McGraw-Hill, New York, 1960), Vol. II, Sec. 17 and Appendix 22.

²See e.g., J. C. Slater, T. M. Wilson, and J. H. Wood, Phys. Rev. **179**, 28 (1969); and A. Rosén and I. Lindgren, *ibid.* **176**, 114 (1968), and references therein.

³J. C. Slater, J. B. Mann, T. M. Wilson, and J. H.

Wood, Phys. Rev. **184**, 672 (1969).

⁴J. C. Slater, *Advan. Quantum Chem.* (to be published), and references therein.

⁵P. A. M. Dirac, Proc. Cambridge Phil. Soc. **26**, 376 (1930); R. Gaspar, *Acta Phys. Hung.* **3**, 263 (1954); W. Kohn and L. J. Sham, Phys. Rev. **140A**, 1133 (1965).

⁶Slater has shown that it is possible to derive a potential of $\rho^{1/3}$ type without use of the uniform electron-gas model by means of simple dimensional arguments regarding the Fermi hole (see, e.g., Ref. 4). However, for our purpose the electron-gas picture is more suitable, and we shall use that in the following.

⁷Hartree atomic units are used throughout this paper. Therefore, the energy is expressed in units of two

rydbergs or 27.21 eV (hartree unit).

⁸I. Lindgren, Phys. Letters **19**, 382 (1965); Arkiv Fysik **31**, 59 (1966); E. A. Kmetko, Phys. Rev. A **1**, 37 (1970); J. H. Wood, Intern. J. Quantum Chem. **35**, 747 (1970).

⁹T. M. Wilson, J. H. Wood, and J. C. Slater, Phys.

Rev. A **2**, 620 (1970); K. Schwarz (unpublished).

¹⁰M. Berrondo and O. Goscinski, Phys. Rev. **184**, 10 (1969).

¹¹I. Lindgren, Intern. J. Quantum Chem. **S5** (1971); I. Lindgren and A. Rosén (unpublished).

PHYSICAL REVIEW A

VOLUME 5, NUMBER 2

FEBRUARY 1972

g_J Values of the $5d[\frac{7}{2}]_{4,3}$ and $5d[\frac{3}{2}]_2$ States in Xe and Hyperfine Structure of the $5d[\frac{7}{2}]_4$ State in $^{129}\text{Xe}^\dagger$

Michael H. Prior and Charles E. Johnson

Department of Physics and Lawrence Berkeley Laboratory,
University of California, Berkeley, California 94720

(Received 4 October 1971)

A magnetic-resonance technique has been used to make an accurate measurement of the g_J values of the $5d[\frac{7}{2}]_4$, $5d[\frac{7}{2}]_3$, and $5d[\frac{3}{2}]_2$ states in xenon and of the hyperfine structure of the $5d[\frac{7}{2}]_4$ state in ^{129}Xe . The $5d$ states are excited and aligned by unidirectional electron impact in a hot-cathode discharge tube containing Xe at a pressure of about 5×10^{-3} Torr. Induced transitions between magnetic sublevels of the aligned $5d$ state are detected by monitoring the intensity of linearly polarized light emitted during the second step in the cascade $5d \rightarrow 6p \rightarrow 6s$. The g_J values were measured by determining the Zeeman transition frequency of a particular $5d$ state in a magnetic field of about 20 G which had been locked to the Zeeman resonance in the $6s[\frac{3}{2}]_2$ metastable state. The results are $g_J = 1.2506(3)$ for $5d[\frac{7}{2}]_4$, $g_J = 1.0749(4)$ for $5d[\frac{7}{2}]_3$, and $g_J = 1.3750(3)$ for $5d[\frac{3}{2}]_2$. The hyperfine structure was measured by placing the tube in a TE_{102} microwave cavity and observing direct ($\Delta F = 1$) hyperfine transitions in a magnetic field of a few gauss. The result for ^{129}Xe in the $5d[\frac{7}{2}]_4$ state is $a = -583.571(2)$ MHz. The error for both the g_J values and the hyperfine structure arises from the magnetic field measurement and corresponds to about one-tenth of the linewidth. Our results are improvements of previous optical measurements.

I. INTRODUCTION

Many of the states with $J \neq 1$ arising from the $5p^5 5d$ configuration in xenon have relatively long radiative lifetimes ($\geq 10^{-5}$ sec). This is due to the nearness ($\approx 2000 \text{ cm}^{-1}$) of the $5p^5 6p$ states to which they decay. Their long lifetimes allow the build-up of large population inversions, which account for the strong infrared laser lines connecting the $5d$ and $6p$ states. In this experiment we have taken advantage of these long lifetimes to make precision magnetic-resonance studies of three $5d$ states: $5d[\frac{7}{2}]_4$, $5d[\frac{7}{2}]_3$, and $5d[\frac{3}{2}]_2$. The technique used is that of magnetic resonance following electron-impact excitation and alignment. This method was first demonstrated by Dehmelt¹ using Hg and was extensively applied to the study of He by Lamb and co-workers.² Since these pioneering investigations, the technique has been used to study the excited states of many atoms as well as a few ions and molecules; much of this work has been summarized by Pebay-Peyroula.³ The $7p[\frac{3}{2}]_2$ and $7p[\frac{3}{2}]_3$ states of xenon have been studied by Chenevier⁴ using this technique.

In particular, we have measured the Landé g factors for the three $5d$ states listed above and

also the hyperfine structure (hfs) of the $5d[\frac{7}{2}]_4$ state in ^{129}Xe ($I = 1/2$). Our results represent improvements of previous optical measurements of the hfs by Liberman,⁵ and of the g_J values by Schlossberg and Javan.⁶

II. METHOD

The Xe energy levels relevant to this experiment are shown in Fig. 1. It is seen that the $5p^5 5d$ states can be produced by electron bombardment with a threshold of about 10 eV. For illustrating the technique, we can limit discussion to the $5d[\frac{7}{2}]_4$ state. The decay path for this state is the two-photon cascade $5d[\frac{7}{2}]_4 \rightarrow 6p[\frac{5}{2}]_3 \rightarrow 6s[\frac{3}{2}]_2$ with $\lambda_1 = 55\,750 \text{ \AA}$ and $\lambda_2 = 8819 \text{ \AA}$. As is known,³ unidirectional electron bombardment near threshold produces an aligned excited state, i. e., Zeeman sublevels with different $|m_J|$, have different probabilities of excitation and consequently different populations. Following excitation, this alignment manifests itself in the polarization and anisotropy of the decay radiation. Since alignment is transferred to the intermediate state by the first step in the cascade, radiation emitted in the second step will also exhibit polarization and anisotropy. Therefore, changes in the populations of the $5d$